COMMUN. MATH. SCI.
Vol. 15, No. 3, pp. 693–710

A TIME INTEGRATION METHOD OF APPROXIMATE FUNDAMENTAL SOLUTIONS FOR NONLINEAR POISSON-TYPE BOUNDARY VALUE PROBLEMS*

COREY JONES† AND HAIYAN TIAN‡

Abstract. A time-dependent method is coupled with the method of approximate particular solutions (MAPS) and the method of approximate fundamental solutions (MAFS) of Delta-shaped basis functions to solve a nonlinear Poisson-type boundary value problem on an irregular shaped domain. The problem is first converted into a sequence of time-dependent nonhomogeneous modified Helmholtz boundary value problems through a fictitious time integration method. Then the superposition principle is applied to split the numerical solution at each time step into an approximate particular solution and a homogeneous solution. A Delta-shaped basis function is used to provide an approximation of the source function at each time step. This allows for an easy derivation of an approximate particular solution. The corresponding homogeneous boundary value problem is solved using MAFS, and also with the method of fundamental solutions (MFS) for comparison purposes. Numerical results support the accuracy and validity of this computational method.

Keywords. fictitious time; nonlinear Poisson-type equations; Delta-shaped basis; modified Helmholtz equation; approximate particular solutions; approximate fundamental solutions

AMS subject classifications. 65N35; 65N80.

1. Introduction

There has been increased research and study over the last several decades in developing computational methods for finding numerical solutions of partial differential equations (PDEs) in general. These methods are either mesh-based methods or meshfree methods. Traditional methods such as the finite-element methods (FEM), finite-difference methods (FDM), and finite-volume methods (FVM) are mesh-based methods. They require a mesh to connect nodes inside the computational domain or on the boundary. Alternatively, meshfree methods such as the radial basis functions (RBFs) method [2, 3], the method of fundamental solutions (MFS) [6], and a boundary method of trefftz type using approximate trial functions [15] to name a few, do not require discretization of the computational domain or boundary.

Numerical techniques of meshfree methods have also been developed over the last decade in the field of solving nonlinear PDEs. As a few examples, Wordelman, Aluru and Ravaioli [22] implemented the finite point method with a weighted least squares fit of the unknown solution using a set of monomial base interpolating functions to solve the 2D and 3D nonlinear semiconductor Poisson equation. Liu [8, 10] solved quasilinear elliptic boundary value problems by a fictitious time integration method (FTIM). Later Tsai, Liu and Yeih [21] used FTIM when incorporating the MFS and Chebyshev polynomials to solve nonlinear Poisson-type PDEs. Reutskiy [18] utilized the method of approximate particular solutions (MAPS) of RBFs and the dual reciprocity method (DRM) together with the MFS to solve nonlinear Poisson-type equations.

Poisson equation is a partial differential equation of elliptic type typically used to model diffusion and it has applications in electrostatics, mechanical engineering, theoretical physics, mesh editing in computer graphics, surface reconstruction, etc. In

*Received: August 26, 2015; accepted (in revised form): July 23, 2016. Communicated by Shi Jin.
†Department of Mathematics, Jones County Junior College, Ellisville, MS 39437, USA (corey.jones@jcjc.edu).
‡Department of Mathematics, The University of Southern Mississippi, Hattiesburg, MS 39406, USA (haiyan.tian@usm.edu).

this paper we consider the general nonlinear Poisson-type boundary value problem

$$-\nabla^2 u(x,y) = H(x,y,u,u_x,u_y), \text{ for } (x,y) \in \Omega, \tag{1.1}$$

$$u(x,y) = f(x,y), \text{ for } (x,y) \in \partial\Omega_D, \tag{1.2}$$

$$\frac{\partial u(x,y)}{\partial \eta} = g(x,y), \text{ for } (x,y) \in \partial\Omega_N, \tag{1.3}$$

where $\nabla^2 = \partial^2/\partial x^2 + \partial^2/\partial y^2$ is the Laplacian operator, Ω is a computational domain with boundary $\partial\Omega$, $\partial\Omega_D$ and $\partial\Omega_N$ denote respectively the Dirichlet and Neumann boundary partitions with $\partial\Omega_D \cup \partial\Omega_N = \partial\Omega$ and $\partial\Omega_D \cap \partial\Omega_N = \varnothing$, η is the unit outward normal with respect to $\partial\Omega$, and H, f, and g are known functions.

Through the FTIM, the problem (1.1)–(1.3) is first transformed into a time-dependent quasilinear problem via a fictitious time, and by numerical integration it is then converted to a sequence of time-dependent linear nonhomogeneous modified Helmholtz boundary value problems. The principle of superposition is then applied to split the numerical solution at each time step into an approximate particular solution and a homogeneous solution. A Delta-shaped basis function, which can handle scattered data in various domains, is used to provide an approximation of the source function at each time step. This allows for an easy derivation of an approximate particular solution of the nonhomogeneous modified Helmholtz equation using the MAPS. The corresponding homogeneous boundary value problem is solved using the MAFS at each time-step. The MAFS does not require a closed form of the fundamental solutions of an elliptic differential operator. So this method can be extended to solving a more geneal type of nonlinear elliptic partial differential equations.

This paper is organized as follows. In Section 2, using FTIM the nonlinear Poisson-type boundary value problem (1.1)–(1.3) is converted into a sequence of time-dependent linear nonhomogeneous modified Helmholtz equations. In Section 3, the MAPS by Delta-shaped basis functions for an approximate particular solution at each time step is provided. In Section 4, the MAFS for solving the associated homogeneous problem at each time step is presented followed by the MFS in Section 5 for comparison with the MAFS. Numerical results for nonlinear Poisson-type problems on various shaped domains are presented in Section 6. The conclusions drawn from the work and numerical results are given in Section 7.

2. Conversion using fictious time integration method

The fictitious time integration method was first developed by Liu and Atluri [11] for solving a large system of nonlinear algebraic equations, and since then it has been used for solving various boundary value problems [8, 9, 10, 12, 21]. We apply this method in our solution process. First, a fictitious time is introduced to convert the nonlinear Poisson-type problem (1.1)–(1.3) into a time-dependent quasilinear problem. Second, numerical integration is performed on the time-dependent quasilinear problem to obtain a sequence of linear nonhomogeneous modified Helmholtz boundary value problems.

A time-dependent function $w(x,y,t)$ is defined as

$$w(x,y,t) = u(x,y)q(t), \tag{2.1}$$

or equivalently as

$$u(x,y,t) = \frac{w(x,y,t)}{q(t)}, \tag{2.2}$$

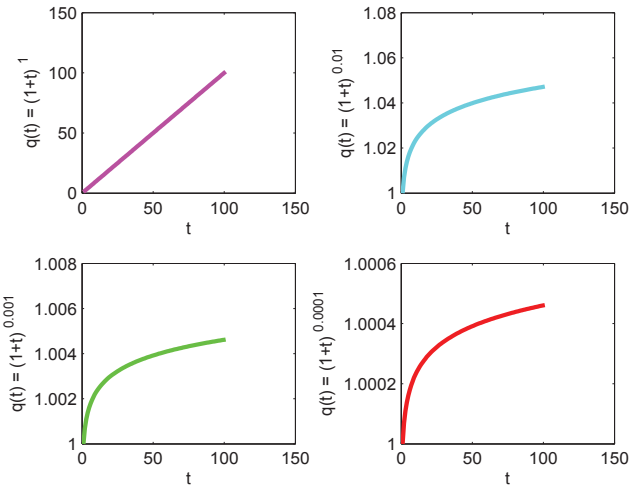

FIG. 2.1. *Plot of the time function* $q(t)=(1+t)^{\beta}$ *with various* β

where t is a fictitious time and $q(t)$ is a time function

$$q(t)=(1+t)^{\beta}, \tag{2.3}$$

with $0<\beta\leq 1$, a parameter for the convergence of the time integration method.

Figure 2.1 displays the plot of $q(t)$ for different values of β. It is noted that the time function is differentiable, $q(0)=1$, and $\lim_{t\to\infty} q(t)=\infty$. The time function $q(t)$ was formulated in [7] and [13] as a new time function as opposed to the time function with $\beta=1$. This new time function was implemented by Tsai, et al [21]. Differentiating (2.1) with respect to t and utilizing Equations (1.1) and (2.2), it can be shown that

$$\frac{\partial w}{\partial t}-\nabla^2\left(\frac{w}{q}\right)=\frac{w}{q}\frac{dq}{dt}+H\left(x,y,\frac{w}{q},\frac{w_x}{q},\frac{w_y}{q}\right),$$

which results in

$$\frac{\partial u}{\partial t}-\frac{1}{q}\nabla^2 u=\frac{1}{q}H(x,y,u,u_x,u_y), \tag{2.4}$$

a time-dependent quasilinear equation of u.

Next a forward Euler integration technique is implemented to integrate Equation (2.4) with $\partial u/\partial t$ being approximated as follows:

$$\frac{\partial u}{\partial t}\approx\frac{u^{I+1}-u^I}{\Delta t}=\frac{u(x,y,t^{I+1})-u(x,y,t^I)}{\Delta t}.$$

Hence, Equation (2.4) becomes

$$\frac{u^{I+1}-u^I}{\Delta t}-\frac{1}{q}\nabla^2 u^{I+1}=\frac{1}{q}H(x,y,u^I,u_x^I,u_y^I), \tag{2.5}$$

which is approximated by

$$\frac{q^{I+1}u^{I+1}}{\Delta t}-\frac{q^I u^I}{\Delta t}-\nabla^2 u^{I+1}=H\left(x,y,u^I,u_x^I,u_y^I\right).$$

This leads to

$$\nabla^2 u^{I+1}(x,y,t) - \frac{q^{I+1}(t)}{\Delta t} u^{I+1}(x,y,t) = -\frac{q^I(t)}{\Delta t} u^I(x,y,t) - H\left(x,y,u^I,u_x^I,u_y^I\right), \text{ in } \Omega, \tag{2.6}$$

$$u^{I+1}(x,y,t) = f(x,y), \text{ on } \partial\Omega_D, \tag{2.7}$$

$$\frac{\partial u^{I+1}(x,y,t)}{\partial \eta} = g(x,y), \text{ on } \partial\Omega_N, \tag{2.8}$$

for $I = 0,1,2,...$, where $u^I(x,y,t) = u(x,y,t^I)$, $q^I(t) = q(I\Delta t)$, $t^I = I\Delta t$, and Δt is the step size for each time step. With Equations (2.6)–(2.8) now a recursive formulation of (1.1)–(1.3), we need to solve a sequence of nonhomogeneous modified Helmholtz boundary value problems.

The numerical procedure for solving Equations (2.6)–(2.8) begins with a chosen initial value of $u^0(x,y,t)$. During the solution process, Equation (2.6) is integrated from $t = 0$ to some final time $t^n = n\Delta t$. The inequality

$$\| u^{I+1}(x,y,t) - u^I(x,y,t) \|_\infty \ < \ \varepsilon \tag{2.9}$$

is used as the criterion to stop the iteration where $\| \bullet \|_\infty$ is the maximum norm and ε is a small positive number.

We note that $0 < \beta \leq 1$ in (2.3) is a parameter for the convergence of the FTIM using a similar scheme as was done in [7, 11], on a system of algebraic equations. Using (2.5), we have

$$u^{I+1} - u^I = \frac{\Delta t}{q}\left[\nabla^2 u^{I+1} + H(x,y,u^I,u_x^I,u_y^I)\right]. \tag{2.10}$$

Now, when the criterion (2.9) is satisfied, u^{I+1} is accepted as the approximate solution to Equations (1.1)–(1.3). To reach the criterion, two possible cases exist for Equation (2.10).

CASE 1: The convergence of $\nabla^2 u^{I+1} + H(x,y,u^I,u_x^I,u_y^I) \to 0$ is relatively fast as $I \to \infty$, and the approximate solution u^{I+1} is obtained.

CASE 2: If the convergence of $\nabla^2 u^{I+1} + H(x,y,u^I,u_x^I,u_y^I) \to 0$ as $I \to \infty$ is slow, a long fictitious time q may be needed to approach the acceptable approximate solution u^{I+1}. Thus, a large $I\Delta t$ may cause q to become a very large value, and as such $1/q \to 0$ as $I \to \infty$ before $\nabla^2 u^{I+1} + H(x,y,u^I,u_x^I,u_y^I) \to 0$.

Hence, the parameter β is to ensure that $\nabla^2 u^{I+1} + H(x,y,u^I,u_x^I,u_y^I) \to 0$ faster than $1/q \to 0$.

3. An approximate particular solution for the nonlinear equation

In order to solve the modified Helmholtz problems in Equations (2.6)–(2.8), the principle of superposition is applied separating the solution $u^{I+1}(x,y,t)$ for each I as

$$u^{I+1}(x,y,t) = u_p^{I+1}(x,y,t) + u_h^{I+1}(x,y,t),$$

where an approximate particular solution $u_p^{I+1}(x,y,t)$ satisfies

$$\nabla^2 u_p^{I+1}(x,y,t) - \frac{q^{I+1}(t)}{\Delta t} u_p^{I+1}(x,y,t) = -\frac{q^I(t)}{\Delta t} u^I(x,y,t) - H\left(x,y,u^I,u_x^I,u_y^I\right), \tag{3.1}$$

and the homogeneous solution $u_h^{I+1}(x,y,t)$ satisfies

$$\nabla^2 u_h^{I+1}(x,y,t) - \frac{q^{I+1}(t)}{\Delta t} u_h^{I+1}(x,y,t) = 0, \text{ in } \Omega, \tag{3.2}$$

$$u_h^{I+1}(x,y,t) = f(x,y) - u_p^{I+1}(x,y,t), \text{ on } \partial\Omega_D, \tag{3.3}$$

$$\frac{\partial u_h^{I+1}(x,y,t)}{\partial \eta} = g(x,y) - \frac{\partial u_p^{I+1}(x,y,t)}{\partial \eta}, \text{ on } \partial\Omega_N, \tag{3.4}$$

for $I = 0,1,2,....$

In the formulation (3.2)–(3.4), the influence of the right hand side of Equation (2.6) on the solution $u^{I+1}(x,y,t)$ has in essence been transferred to the boundary for each I. In order to derive an accurate approximation to the particular solution $u_p^{I+1}(x,y,t)$ in Equation (3.1) for each time step I, it is necessary to find an accurate approximation of the source function

$$h^I(x,y,t) = -\frac{q^I(t)}{\Delta t} u^I(x,y,t) - H\left(x,y,u^I,u_x^I,u_y^I\right). \tag{3.5}$$

It is also important that a closed form approximate particular solution $u_p^{I+1}(x,y,t)$ can be easily derived after the source function approximation is obtained. Two-dimensional Delta-shaped basis functions $I_{M,\chi}(x,y;\xi,\eta)$ are used for this purpose because of their specific characteristics [16, 19, 20]. A 2D Delta-shaped basis function is given as

$$I_{M,\chi}(x,y;\xi,\eta) = \sum_{n=1}^{M}\sum_{m=1}^{M} c_{n,m}(\xi,\eta)\varphi_n(x)\varphi_m(y), \tag{3.6}$$

where

$$c_{n,m}(\xi,\eta) = r_n(M,\chi) r_m(M,\chi)\varphi_n(\xi)\varphi_m(\eta). \tag{3.7}$$

The φ_n are the eigenfunctions of the following Sturm–Liouville problem on the interval $[-1,1]$,

$$-\varphi'' = \lambda\varphi, \tag{3.8}$$

$$\varphi(-1) = \varphi(1) = 0. \tag{3.9}$$

The eigenfunctions and eigenvalues of the problem (3.8)–(3.9) are

$$\varphi_n(x) = \sin\left(\frac{n\pi(x+1)}{2}\right) \text{ and } \lambda_n = \left(\frac{n\pi}{2}\right)^2,\ n = 1,2,3,....$$

The regularizing coefficients $r_n(M,\chi)$ are determined by the Riesz regularization technique [15, 19] with

$$r_n(M,\chi) = \left(1 - \frac{\lambda_n}{\lambda_{M+1}}\right)^{\chi} = \left[1 - \left(\frac{n}{M+1}\right)^2\right]^{\chi},$$

where the parameters M and χ are positive integers with M playing the role of scaling and χ playing the role of regularization. The coupled parameters are taken as:

$$\chi = 4,6,9,14,22,$$

$$M = 10, 20, 30, 50, 100.$$

Now to approximate Equation (3.5), for each time step I, which will be sampled at the scattered data points $\{(x_i, y_i)\}_{i=1}^{N}$ in $\mathbb{R}^2$, a linear combination of the 2D Delta-shaped basis functions is used. To improve the accuracy of the approximation of Equation (3.5), translates of Delta-shaped basis functions of two different shapes are used. Thus, the approximate source function takes the form

$$\widetilde{h}^I(x,y,t) = \sum_{j=1}^{K_1} p_j I_{M_1,\chi_1}(x,y;\xi_j,\eta_j) + \sum_{j=K_1+1}^{K_1+K_2} p_j I_{M_2,\chi_2}(x,y;\xi_j,\eta_j) \tag{3.10}$$

where

$$\psi_1 = \sum_{j=1}^{K_1} p_j I_{M_1,\chi_1}(x,y;\xi_j,\eta_j) \tag{3.11}$$

is the contribution of the type-one basis functions, and

$$\psi_2 = \sum_{j=K_1+1}^{K_1+K_2} p_j I_{M_2,\chi_2}(x,y;\xi_j,\eta_j) \tag{3.12}$$

is the contribution of type-two basis functions. Let $K = K_1 + K_2$, then $\{p_j\}_{j=1}^{K}$ are the unknown coefficients to be determined, and $\{(\xi_j, \eta_j)\}_{j=1}^{K}$ are the center points randomly chosen from the interior of the domain.

We now derive an approximate particular solution $u_p^{I+1}(x,y,t)$ for each I satisfying Equation (3.1). Under the framework of the dual reciprocity method (DRM) [14], after approximating the source function, an approximate particular solution associated with the Delta-shaped basis functions $I_{M,\chi}(x,y;\xi,\eta)$ is required. That is, for each I a function $\Psi^{I+1}(x,y,t;\xi,\eta)$ is desired satisfying

$$\nabla^2 \Psi^{I+1} - \frac{q^{I+1}}{\Delta t} \Psi^{I+1} = I_{M,\chi}(x,y;\xi,\eta) = \sum_{n=1}^{M}\sum_{m=1}^{M} c_{n,m}(\xi,\eta)\varphi_n(x)\varphi_m(y).$$

The function $\Psi^{I+1}(x,y,t;\xi,\eta)$ can be found to be

$$\Psi^{I+1}(x,y,t;\xi,\eta) = -\sum_{n=1}^{M}\sum_{m=1}^{M} \frac{r_n(M,\chi) r_m(M,\chi)\varphi_n(\xi)\varphi_m(\eta)\varphi_n(x)\varphi_m(y)}{\lambda_n + \lambda_m + \frac{q^{I+1}(t)}{\Delta t}}.$$

Since the source function (3.5) is approximated by (3.10) as a linear combination of two types of Delta-shaped basis functions, an approximate particular solution $u_p^{I+1}(x,y,t)$ can be represented as

$$\Phi^{I+1}(x,y,t) = -\left[\Phi_1^{I+1}(x,y,t) + \Phi_2^{I+1}(x,y,t)\right],$$

where

$$\Phi_1^{I+1}(x,y,t) = \sum_{j=1}^{K_1}\sum_{n=1}^{M_1}\sum_{m=1}^{M_1} \frac{p_j r_n(M_1,\chi_1) r_m(M_1,\chi_1)\varphi_n(\xi_j)\varphi_m(\eta_j)\varphi_n(x)\varphi_m(y)}{\lambda_n + \lambda_m + \frac{q^{I+1}(t)}{\Delta t}},$$

$$\Phi_2^{I+1}(x,y,t) = \sum_{j=K_1+1}^{K_1+K_2}\sum_{n=1}^{M_2}\sum_{m=1}^{M_2} \frac{p_j r_n(M_2,\chi_2) r_m(M_2,\chi_2)\varphi_n(\xi_j)\varphi_m(\eta_j)\varphi_n(x)\varphi_m(y)}{\lambda_n + \lambda_m + \frac{q^{I+1}(t)}{\Delta t}},$$

corresponding to Equations (3.11) and (3.12), respectively.

4. Approximate fundamental solutions for the homogeneous problem

The method of fundamental solutions has been widely used for solving elliptic boundary value problems such as Equations (3.2)–(3.4). The MFS is a flexible and efficient meshless boundary method [1, 4, 5, 6]. However, it requires a closed form fundamental solution of the differential operator be known in order to construct an approximate solution of the problem. The method of approximate fundamental solutions [15, 17, 19] can circumvent this limitation by not requiring a known closed form fundamental solution. The Delta-shaped basis functions (3.6) are used to obtain the approximate fundamental solutions of the differential operator in Equation (3.2).

An approximate fundamental solution of an elliptic differential operator $\mathcal{L}$ is a function $R(x,y;\xi,\eta)$ satisfying

$$\mathcal{L}R(x,y;\xi,\eta) = -I_{M,\chi}(x,y;\xi,\eta).$$

The homogeneous solution $u_h^{I+1}(x,y,t)$ at each time step is expressed as a linear combination of approximate fundamental solutions

$$u_h^{I+1}(x,y,t) = \sum_{j=1}^{K} c_j R^{I+1}(x,y,t;\xi_j,\eta_j), \text{ for } (x,y)\in\Omega\cup\partial\Omega,$$

where R^{I+1} is the approximate fundamental solution for Equation (3.2) at that time step and it is represented as

$$R^{I+1}(x,y,t;\xi,\eta) = \sum_{n=1}^{M}\sum_{m=1}^{M} \frac{r_n(\alpha)r_m(\alpha)\varphi_n(\xi)\varphi_m(\eta)\varphi_n(x)\varphi_m(y)}{\lambda_n+\lambda_m+\frac{q^{I+1}(t)}{\Delta t}}.$$

Now the homogeneous solution $u_h^{I+1}(x,y,t)$ satisfies the boundary conditions at the boundary collocation points resulting in the following system of equations

$$\sum_{j=1}^{K} c_j R^{I+1}(x_i,y_i,t;\xi_j,\eta_j) = f(x_i,y_i) - u_p^{I+1}(x_i,y_i,t), \text{ for } i=1,...,N_1,$$

$$\sum_{j=1}^{K} c_j \frac{\partial R^{I+1}(x_i,y_i,t;\xi_j,\eta_j)}{\partial n} = g(x_i,y_i) - \frac{\partial u_p^{I+1}(x_i,y_i,t)}{\partial_\eta}, \text{ for } i=N_1+1,...,N_1+N_2,$$

where N_1 points $\{(x_i,y_i)\}_{i=1}^{N_1}$ are chosen on $\partial\Omega_D$ and another set of N_2 points $\{(x_i,y_i)\}_{i=N_1+1}^{N_1+N_2}$ chosen on $\partial\Omega_N$. The Abel regularization technique is utilized here for the regularizing coefficients r_n in Equation (3.7) which are set as $r_n(\alpha)=e^{-\alpha\lambda_n}$, with α being the time moment. More detailed discussion on the regularization factors can be found in [15, 19]. The values of α and M are coupled parameters which are chosen as follows in the calculation,

$$\begin{aligned}
\alpha\epsilon[0.005,0.01], &\text{ for } M\le 30,\\
\alpha\epsilon[0.001,0.005], &\text{ for } 30<M\le 50,\\
\alpha\epsilon[0.0012,0.0015], &\text{ for } 50<M\le 100.
\end{aligned}$$

The derivative in the outward normal direction of $\partial\Omega$ is

$$\frac{\partial F}{\partial n} = \nabla F\cdot\overrightarrow{J},$$

where $\overrightarrow{J}$ is a unit outward normal vector at a given point $(x(t),y(t))$ on $\partial\Omega$, and

$$\overrightarrow{J}=\frac{<y',-x'>}{\sqrt{(x')^2+(y')^2}}.$$

5. Fundamental solutions for the homogeneous problem

For comparisons with MAFS, we present the method of fundamental solutions to solve the time-dependent boundary value problem (3.2)–(3.4). A fundamental solution of a differential operator $\mathcal{L}$ is a function $G(x,y;\xi,\eta)$ satisfying

$$\mathcal{L}G(x,y;\xi,\eta)=-\delta(x,y;\xi,\eta),$$

where $\delta(x,y;\xi,\eta)$ denotes the Dirac delta function. The homogeneous solution $u_h^{I+1}(x,y,t)$ at each time step is expressed as a linear combination of fundamental solutions

$$u_h^{I+1}(x,y,t)=\sum_{j=1}^{K}b_jG^{I+1}(x,y,t;\xi_j,\eta_j),\ \text{for}\ (x,y)\in\Omega\cup\partial\Omega,$$

where G^{I+1} is the fundamental solution for Equation (3.2) at that time step and is represented as

$$G^{I+1}(x,y,t;\xi,\eta)=K_0\left(\sqrt{\frac{q^{I+1}(t)}{\Delta t}}\,|(x,y)-(\xi,\eta)|\right).$$

K_0 is the modified Bessel function of the second kind of order zero.

Now the homogeneous solution $u_h^{I+1}(x,y,t)$ satisfies the boundary conditions at the boundary collocation points resulting in the following system of equations

$$\sum_{j=1}^{K}b_jG^{I+1}(x_i,y_i,t;\xi_j,\eta_j)=f(x_i,y_i)-u_p^{I+1}(x_i,y_i,t),\ \text{for}\ i=1,...,N_1,$$

$$\sum_{j=1}^{K}b_j\frac{\partial G^{I+1}(x_i,y_i,t;\xi_j,\eta_j)}{\partial n}=g(x_i,y_i)-\frac{\partial u_p^{I+1}(x_i,y_i,t)}{\partial_\eta},\ \text{for}\ i=N_1+1,...,N_1+N_2,$$

where N_1 points $\{(x_i,y_i)\}_{i=1}^{N_1}$ are chosen on $\partial\Omega_D$ and another set of N_2 points $\{(x_i,y_i)\}_{i=N_1+1}^{N_1+N_2}$ chosen on $\partial\Omega_N$.

6. Numerical results

In order to measure the accuracy and validity of the proposed method for solving the nonlinear Poisson-type differential equations, we provide numerical examples in this section. To measure the accuracy of the approximate solution at each time step, we use the mean square root error MSE defined as follows,

$$MSE=\sqrt{\frac{1}{N_t}\sum_{k=1}^{N_t}[\widetilde{u}(x_k,y_k,t)-u(x_k,y_k)]^2}$$

where $\widetilde{u}$, the numerical solution at each time step, is compared with the exact analytical solution u. The test points $\{(x_k,y_k)\}_{k=1}^{N_t}$ are the points used for collocation inside the domain.

EXAMPLE 6.1. Consider the Poisson-type nonlinear problem

$$-\nabla^2 u(x,y) = -4u^3(x,y), \text{ for } (x,y) \in \Omega, \tag{6.1}$$

$$u(x,y) = \frac{1}{4+x+y}, \text{ for } (x,y) \in \partial\Omega, \tag{6.2}$$

where the computational domain is a square given as $\Omega = \{(x,y) \mid |x| \le \frac{1}{2} \wedge |y| \le \frac{1}{2}\}$. The exact analytical solution is $u(x,y) = 1/(4+x+y)$. For this example, we choose 100 of the type 1 basis centers and 125 of the type 2 basis centers randomly inside the domain as shown in Figure 6.1. The number of interior collocation points is 450, twice the total number of basis centers. There are 32 points collocated on the square boundary with 8 points on each side of the square. The number of source points is 28, chosen on $\widehat{\partial\Omega}$ which is a circle centered at the origin with a radius of 0.9 for MAFS and 3 for MFS. The arbitrarily chosen initial solution for $I = 0$ is the constant function $u^0 = 1$. There are 500 time steps recorded. Figures 6.2–6.5 display the error status of the approximate solution for different Δt with $\beta = 10^{-2}$ and $\beta = 10^{-4}$. The iteration corresponding to a larger Δt tends to converge faster. The numerical results are more accurate for smaller values of β.

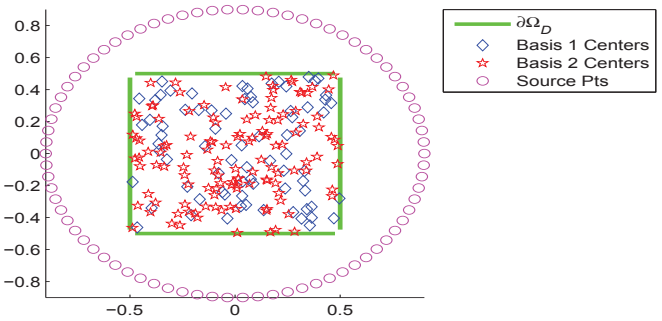

FIG. 6.1. *(Example 6.1) Square Domain, Boundary, Basis Centers, and Source Points*

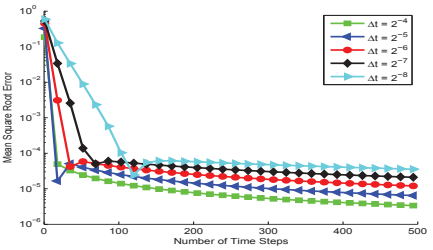

FIG. 6.2. *(Example 6.1) Time function:* $\beta = 10^{-2}$, *Basis 1:* $M = 10$ *and* $\chi = 4$, *Basis 2:* $M = 30$ *and* $\chi = 9$, *MAFS:* $\alpha = 0.0012$ *and* $M = 100$.

EXAMPLE 6.2. To demonstrate the flexibility of the method, we now consider a nonlinear Poisson-type problem in [18] which includes the spatial variables x, y in the

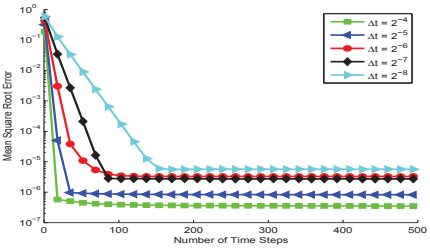

FIG. 6.3. *(Example 6.1) Time function:* $\beta = 10^{-4}$, *Basis 1:* $M = 10$ *and* $\chi = 4$, *Basis 2:* $M = 30$ *and* $\chi = 9$, *MAFS:* $\alpha = 0.0012$ *and* $M = 100$.

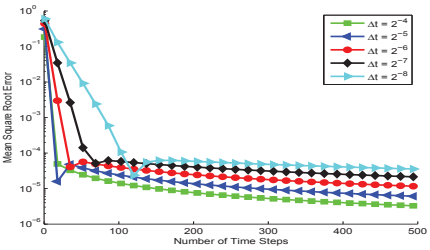

FIG. 6.4. *(Example 6.1) Time function:* $\beta = 10^{-2}$, *Basis 1:* $M = 10$ *and* $\chi = 4$, *Basis 2:* $M = 30$ *and* $\chi = 9$, *MFS*

source function given as

$$-\nabla^2 u(x,y) = -(u^2 + 6x - x^6 - 4x^4 y - 4x^2 y^2), \text{ for } (x,y) \in \Omega, \tag{6.3}$$

$$u(x,y) = x^3 + 2xy, \text{ for } (x,y) \in \partial\Omega. \tag{6.4}$$

The computational domain Ω is ameba shaped, which is bounded by the curve

$$x(t) = \rho(t)\cos t,\ y(t) = \rho(t)\sin t,$$

with

$$\rho(t) = \exp(\sin\theta)\sin^2(2\theta) + \exp(\cos\theta)\cos^2(2\theta),\ 0 \le t \le 2\pi.$$

The exact analytical solution is $u(x,y) = x^3 + 2xy$. To ensure that the domain lies within $[-0.5,0.5] \times [-0.5,0.5]$ for the Delta-shaped basis functions, the problem (6.3)–(6.4) is transformed into a problem on a new domain $\Omega' = \{(x',y') | x' = \rho' \cos t,\ y' = \rho' \sin t\}$ where $x',\ y' \in [-0.5,0.5]$ and

$$x'(t) = -\frac{1}{10} + \rho'(t)\cos t,\ y'(t) = -\frac{1}{10} + \rho'(t)\sin t, \tag{6.5}$$

$$\rho'(t) = \frac{1}{5}\left[\exp(\sin\theta)\sin^2(2\theta) + \exp(\cos\theta)\cos^2(2\theta)\right],\ 0 \le t \le 2\pi. \tag{6.6}$$

There are 25 of the type 1 basis centers and 75 of the type 2 basis centers randomly chosen inside the domain as displayed in Figure 6.6. The number of inner collocation

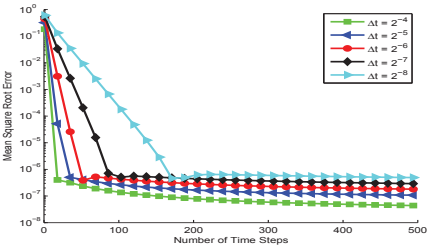

FIG. 6.5. *(Example 6.1) Time function:* $\beta = 10^{-4}$, *Basis 1:* $M = 10$ *and* $\chi = 4$, *Basis 2:* $M = 30$ *and* $\chi = 9$, *MFS*

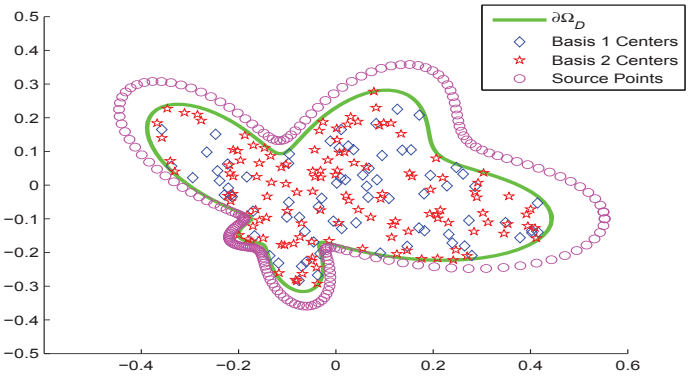

FIG. 6.6. *(Example 6.2) Ameba Domain, Boundary, Basis Centers, and Source Points*

points used is 200, twice the total number of basis centers. There are 200 points collocated on the boundary and 100 source points on the fictitious boundary $\widehat{\partial\Omega}$ which is defined according to (6.5)–(6.6) with $\rho'(t)$ multiplied by 1.65. The arbitrarily chosen initial solution for $I = 0$ is the constant function $u^0 = 1$. With $\beta = 10^{-2}$ and 10^{-4} as the value of the parameter in the time-like function. Figures 6.7–6.10 display the error profiles for the approximate solution with different Δt. It is again noticed that the iteration corresponding to a larger Δt tends to converge faster and the numerical results are more accurate for smaller β. After 500 time steps, the MSE reaches 3.0406×10^{-5} with $\Delta t = 2^{-4}$ and $\beta = 10^{-2}$ using MAFS. Alternatively using MFS, the MSE reaches 1.7885×10^{-5} with the same choices of β and Δt. The MSE errors for 500 iterations using MAFS and MFS for different parameter values β and Δt are recorded in Table 6.1.

EXAMPLE 6.3. To further demonstrate the applicability of the method, we consider the nonlinear Poisson-type problem that includes in the source function partial derivatives as well as the spacial variables x and y,

$$-\nabla^2 u(x,y) = -4u^3 + \left(\frac{\partial u}{\partial x}\right)^2 + \left(\frac{\partial u}{\partial y}\right)^2 - \frac{2}{(4+x+y)^4}, \text{ for } (x,y) \in \Omega,$$

$$u(x,y) = \frac{1}{4+x+y}, \text{ for } (x,y) \in \partial\Omega.$$

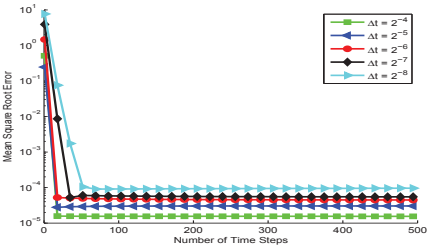

FIG. 6.7. *(Example 6.2) Time function:* $\beta = 10^{-2}$, *Basis 1:* $M = 10$ *and* $\chi = 4$, *Basis 2:* $M = 30$ *and* $\chi = 9$, *MAFS:* $\alpha = 0.0012$ *and* $M = 100$.

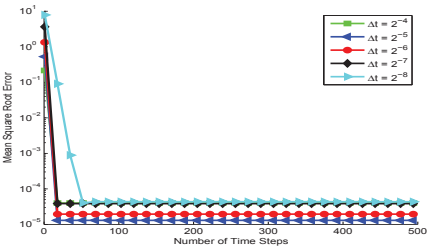

FIG. 6.8. *(Example 6.2) Time function:* $\beta = 10^{-4}$, *Basis 1:* $M = 10$ *and* $\chi = 4$, *Basis 2:* $M = 30$ *and* $\chi = 9$, *MAFS:* $\alpha = 0.0015$ *and* $M = 100$.

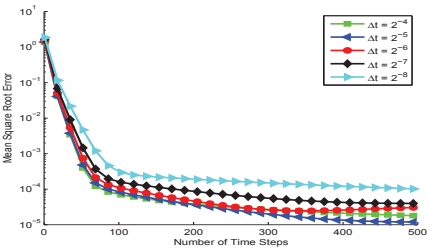

FIG. 6.9. *(Example 6.2) Time function:* $\beta = 10^{-2}$, *Basis 1:* $M = 10$ *and* $\chi = 4$, *Basis 2:* $M = 30$ *and* $\chi = 9$, *MFS*

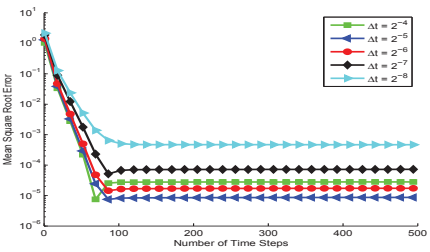

FIG. 6.10. *(Example 6.2) Time function:* $\beta = 10^{-4}$, *Basis 1:* $M = 10$ *and* $\chi = 4$, *Basis 2:* $M = 30$ *and* $\chi = 9$, *MFS*

β	Δt	MAFS_MSE	MFS_MSE
10^{-2}	2^{-4}	$3.0406\cdot10^{-5}$	$1.7885\cdot10^{-5}$
10^{-2}	2^{-5}	$1.5503\cdot10^{-5}$	$1.1946\cdot10^{-5}$
10^{-2}	2^{-6}	$4.4710\cdot10^{-5}$	$3.0844\cdot10^{-5}$
10^{-2}	2^{-7}	$5.4849\cdot10^{-5}$	$3.9772\cdot10^{-5}$
10^{-2}	2^{-8}	$9.5819\cdot10^{-5}$	$1.0094\cdot10^{-4}$
10^{-4}	2^{-4}	$3.9870\cdot10^{-5}$	$2.8045\cdot10^{-5}$
10^{-4}	2^{-5}	$1.2975\cdot10^{-5}$	$8.7097\cdot10^{-6}$
10^{-4}	2^{-6}	$1.9453\cdot10^{-5}$	$1.7369\cdot10^{-5}$
10^{-4}	2^{-7}	$3.8461\cdot10^{-5}$	$7.2623\cdot10^{-5}$
10^{-4}	2^{-8}	$9.4051\cdot10^{-5}$	$4.6944\cdot10^{-4}$

TABLE 6.1. *(Example 6.2) MAFS and MFS Errors for different parameter values after 500 iterations*

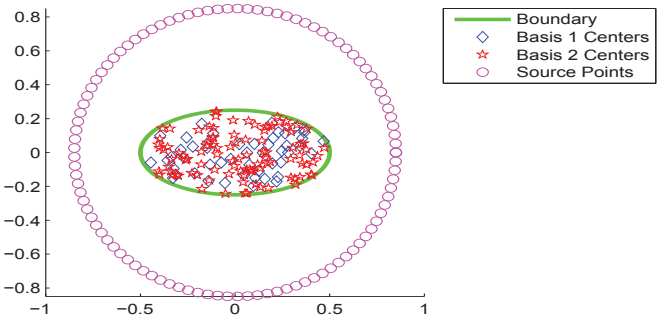

FIG. 6.11. *(Example 6.3) Ellipse Domain, Boundary, Basis Centers, and Source Points*

The computational domain Ω is elliptical with a major axis of 1 and a minor axis of 0.5. Its boundary is defined parametrically as $\Omega=\{(x,y)|x=0.5\cos\theta,\ y=0.25\sin\theta\}$. The exact analytical solution is $u(x,y)=1/(4+x+y)$. There are 100 of the type 1 basis centers and 225 of the type 2 basis centers randomly chosen inside the domain as displayed in Figure 6.11. The number of inner collocation points used is 650, twice the total number of basis centers. There are 50 points collocated on the boundary and 25 source points chosen from the fictitious boundary $\widehat{\partial\Omega}$ which is a circle centered at the origin with a radius of 0.9 for MAFS and 1 for MFS. The arbitrarily chosen initial solution for $I=0$ is again the constant function $u^0=1$. With $\beta=10^{-2}$ and 10^{-4} as the parameter value for the time-like function, Figures 6.12–6.15 detail the error status with different time step sizes. As the value of β gets smaller, the time discretizations with different Δt produce negligible differences in the error results. The MSE reaches 3.1296×10^{-7} and 1.11184×10^{-8} using MAFS and MFS, respectively, after 500 time steps with $\Delta t=2^{-4}$ and $\beta=10^{-4}$.

EXAMPLE 6.4. Finally, to demonstrate the flexibility of the method to problems with mixed boundary conditions, we consider the problem (6.1)–(6.2) redefined with both Dirichlet and Neumann data given on portions of the boundary as

$$-\nabla^2 u(x,y)=-4u^3(x,y),\ \text{for}\ (x,y)\in\Omega,$$

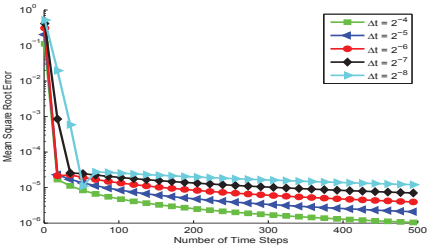

FIG. 6.12. *(Example 6.3) Time Function:* $\beta = 10^{-2}$, *Basis 1:* $M = 10$ *and* $\chi = 4$, *Basis 2:* $M = 20$ *and* $\chi = 6$, *MAFS:* $\alpha = 0.005$ *and* $M = 50$.

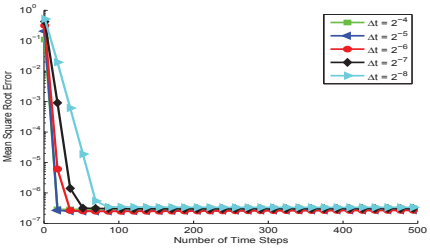

FIG. 6.13. *(Example 6.3) Time Function:* $\beta = 10^{-4}$, *Basis 1:* $M = 10$ *and* $\chi = 4$, *Basis 2:* $M = 20$ *and* $\chi = 6$, *MAFS:* $\alpha = 0.005$ *and* $M = 50$.

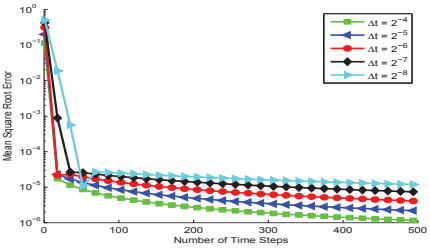

FIG. 6.14. *(Example 6.3) Time Function:* $\beta = 10^{-2}$, *Basis 1:* $M = 10$ *and* $\chi = 4$, *Basis 2:* $M = 20$ *and* $\chi = 6$, *MFS*

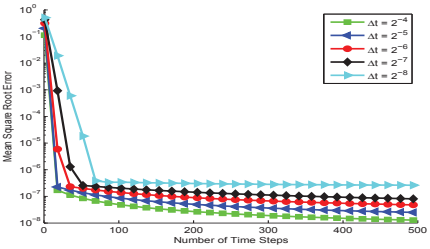

FIG. 6.15. *(Example 6.3) Time Function:* $\beta = 10^{-4}$, *Basis 1:* $M = 10$ *and* $\chi = 4$, *Basis 2:* $M = 20$ *and* $\chi = 6$, *MFS*

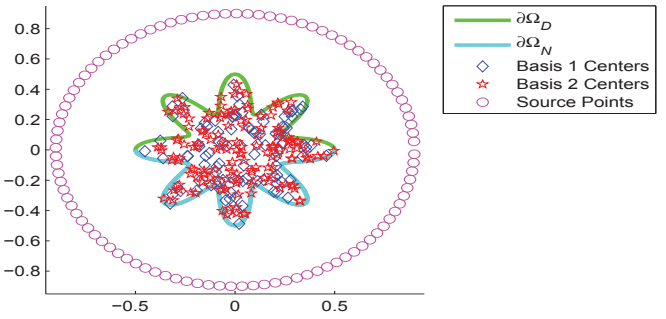

FIG. 6.16. *(Example 6.4) Star Domain, Boundary, Basis Centers, and Source Points*

$$u(x,y) = \frac{1}{4+x+y}, \text{ for } (x,y) \in \partial\Omega_D,$$
$$\frac{\partial u(x,y)}{\partial \eta} = -\frac{x+y}{(4+x+y)^2}, \text{ for } (x,y) \in \partial\Omega_N,$$

on a star shaped domain Ω. The boundary of the domain is parameterized by

$$x(t) = \rho(t)\cos t,\ y(t) = \rho(t)\sin t, \tag{6.7}$$

where

$$\rho(t) = 0.25(1+\cos^2(4t)),\ 0 \le t \le 2\pi. \tag{6.8}$$

The exact analytical solution is $u(x,y) = 1/(4+x+y)$. There are 100 of the type 1 basis centers and 225 of the type 2 basis centers randomly chosen inside the domain as displayed in Figure 6.16. The number of inner collocation points used is 650, twice the total number of basis centers. There are 200 points collocated on the boundary with 100 points on the upper half of the star curve and 100 points on the lower half, and 100 source points chosen from the fictitious boundary $\widehat{\partial\Omega}$ which is a circle centered at the origin with a radius of 0.95 for MAFS and 3 for MFS. The arbitrarily chosen initial solution for $I = 0$ is again the constant function $u^0 = 1$. Figures 6.17–6.20 detail the error status using different time discretizations. The time-like function has $\beta = 10^{-3}$ and $\beta = 10^{-5}$. We again notice that a smaller β value for the time-like function leads to better results, and for the same value of β a larger Δt produces better results. The iteration reaches a remarkable MSE of 4.6924×10^{-9} with MAFS and 1.2257×10^{-9} with MFS when $\beta = 10^{-5}$ and $\Delta t = 2^{-4}$.

The boundary value problem (1.1)–(1.3) is a time-independent problem, and Equations (2.6)–(2.8) is a time-dependent reformulation of the problem (1.1)–(1.3). Our numerical examples reach the steady state solution faster with larger values of Δt within our range of $10^{-5} \le \beta \le 10^{-2}$ and $2^{-8} \le \Delta t \le 2^{-4}$. Smaller values of β causes the time function q to increase slower, and thus, causes $\frac{\Delta t}{q} \to 0$ slower than $\nabla^2 u^{I+1} + H(x,y,u^I,u_x^I,u_y^I) \to 0$ as $I \to \infty$. Since u^{I+1} is accepted as the approximate solution $\widetilde{u}$ at each time step when Equation (2.9) is satisfied, and hence Equation (2.10) holds, the parameter values for β and Δt are chosen to ensure that $\nabla^2 u^{I+1} + H(x,y,u^I,u_x^I,u_y^I) \to 0$ before $\frac{\Delta t}{q} \to 0$ as $I \to \infty$.

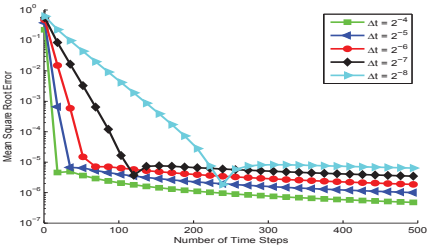

FIG. 6.17. *(Example 6.4) Time Function:* $\beta = 10^{-3}$, *Basis 1:* $M = 10$ *and* $\chi = 4$, *Basis 2:* $M = 20$ *and* $\chi = 6$, *MAFS:* $\alpha = 0.0012$ *and* $M = 100$.

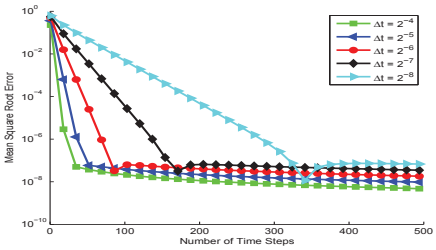

FIG. 6.18. *(Example 6.4) Time Function:* $\beta = 10^{-5}$, *Basis 1:* $M = 10$ *and* $\chi = 4$, *Basis 2:* $M = 20$ *and* $\chi = 6$, *MAFS:* $\alpha = 0.0012$ *and* $M = 100$.

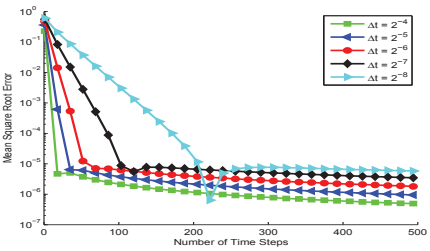

FIG. 6.19. *(Example 6.4) Time Function:* $\beta = 10^{-3}$, *Basis 1:* $M = 10$ *and* $\chi = 4$, *Basis 2:* $M = 20$ *and* $\chi = 6$, *MFS*

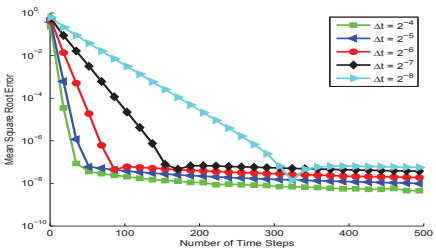

FIG. 6.20. *(Example 6.4) Time Function:* $\beta = 10^{-5}$, *Basis 1:* $M = 10$ *and* $\chi = 4$, *Basis 2:* $M = 20$ *and* $\chi = 6$, *MFS*

7. Conclusion

A general nonlinear Poisson-type boundary value problem is solved with different nonlinear terms on various shaped domains. The fictitious time integration method is performed to transform the nonlinear PDE into a sequence of time-dependent linear nonhomogeneous modified Helmholtz boundary value problems. Delta-shaped basis functions are used to approximate the source function at each time step since the Delta-shaped basis can effectively handle scattered data. An approximate particular solution by Delta-shaped basis functions is obtained at each time level, and the homogeneous boundary value problem at each level is solved using the method of approximate fundamental solutions. For comparison purposes, the MFS was additionally used to solve the homogeneous boundary value problem at each level.

The validity and accuracy of the method are supported with numerical examples with different kinds of source functions and on various domains. The numerical results indicate the computational method is accurate and effective for solving nonlinear Poisson-type PDEs. The errors associated with the approximate solution settle rapidly to a very good accuracy. As such, a reasonable number of time steps can give desired accuracy of the approximate solution. This method circumvents the need for a fundamental solution of the differential operator and hence it is applicable for more general class of partial differential equations.

REFERENCES

[1] A. Bogomolny, *Fundamental solutions method for elliptic boundary value problems*, SIAM J. Numer. Anal., 22(4):644–669, 1985.

[2] E. Kansa, *Application of Hardy multiquadric interpolation to hydro-dynamics*, Simulations 4(19):111–117, 1986.

[3] C. Franke and R. Schaback, *Solving partial differential equations by collocation using radial basis functions*, Appl. Math.Comput., 93(1):73–82, 1998.

[4] C.S. Chen, C.M. Fan, and J. Monroe, *The method of fundamental solutions for solving elliptic partial differential equations with variable coefficients*, in The Method of Fundamental Solutions-A Meshless Method, Dynamics Publisher, 2008.

[5] G. Fairweather and A. Karageorghis, *The method of fundamental solutions for elliptic boundary value problems*, Adv. Comput. Math., 9:69–95, 1998.

[6] V.D. Kupradze and M.A. Aleksidze, *The method of functional equations for the approximate solution of certain boundary value problems*, Comp. Math. and Math. Phys., 4(4):82–126, 1964.

[7] C.Y. Ku, W.C. Yeih, C.S. Liu, and C.C. Chi, *Applications of the fictitious time integration method using a new time-like function*, Comput. Model Eng. Sci., 43:173–190, 2009.

[8] C.S. Liu, *A fictitious time integration method for two-dimensional quasilinear elliptic boundary value problems*, Comput. Model Eng. Sci., 33:179–198, 2008.

[9] C.S. Liu, *A fictitious time integration method for solving M-point boundary value problems*, Comput. Model Eng. Sci., 39:125–154, 2009.

[10] C.S. Liu, *A fictitious time integration method for quasilinear elliptic boundary value problem defined in an arbitrary plane domain*, Comput. Model Eng. Sci., 11:15–32, 2009.

[11] C.S. Liu and S.N. Atluri, *A novel time integration method for solving a large system of non-linear algebraic equations*, Comput. Model Eng. Sci., 31:71–83, 2008.

[12] C.S. Liu and S.N. Atluri, *A novel fictitious time integration method for solving the discretized inverse Sturm-Louiville problems for specified eigenvalues,* Comput. Model Eng. Sci., 36:261–285, 2008.

[13] C.S. Liu and S.N. Atluri, *A fictitious time integration method for the numerical solution of the Fredholm integral equation and for numerical differentiation of noisy data and its relation to the filter theory*, Comput. Model Eng. Sci., 41:243–261, 2009.

[14] D. Nardini and C.A. Brebbia, *A new approach to free vibration analysis using boundary elements*, in Boundary Element Methods in Engineering, Springer–Verlag, New York, 1982.

[15] S. Reutskiy, *A boundary method of trefftz type with approximate trial functions*, Eng. Anal. Bound. Elem., 26:341–353, 2002.

[16] S. Reutskiy, *A boundary method of trefftz type for PDEs with scattered data*, Eng. Anal. Bound.

Elem., 29:713–724, 2005.
[17] S. Reutskiy, *The method of approximate fundamental solutions (MAFS) for elliptic equations of general type with variable coefficients*, Eng. Anal. Bound. Elem., 36:985–992, 2012.
[18] S. Reutskiy, *Method of particular solutions for nonlinear Poisson-type equations in irregular domains*, Eng. Anal. Bound. Elem., 37:401–408, 2013.
[19] S. Reutskiy, C.S. Chen, and H.Y. Tian, *A boundary meshless method using Chebyshev interpolation and trigonometric basis function for solving heat conduction problems*, Int. J. Numer. Meth. Eng., 74:1621–1644, 2008.
[20] H.Y. Tian, S. Reutskiy, and C.S. Chen, *A basis function for approximation and solutions of partial differential equations*, Numer. Methods Part. Diff. Eqs., 24(3):1018–1036, 2007.
[21] C. Tsai, C. Liu, and W. Yeih, *Fictitious time integration method of fundamental solutions with Chebychev polynomials for solving Poisson-type nonlinear PDEs*, Comput. Model Eng. Sci., 56:131–151, 2010.
[22] C.J. Wordelman, N.R. Aluru, and U. Ravaioli, *A meshless method for the numerical solution of the 2- and 3-D semiconductor Poisson equation*, Comput. Model Eng. Sci., 1:121–126, 2000.